ABSORPTION OF 40--70-MeV $\pi^{\pm}$ MESONS BY CARBON IN A PROPANE BUBBLE CHAMBER

M. P. BALANDIN, O. I. IVANOV, V. A. MOISEENKO, and G. L. SOKOLOV

Joint Institute for Nuclear Research

Submitted to JETP editor May 9, 1963

J. Exptl. Theoret. Phys. (U.S.S.R.) **46**, 415-430 (February, 1964)

A 30-cm propane bubble chamber was used to study the absorption of π^{+} and π^{-} mesons having equal energies by carbon nuclei. The total absorption and charge exchange cross sections for π^{+} and π^{-} mesons in carbon nuclei are 98^{+17}_{-10} and 99^{+24}_{-19} mb, respectively. The angular distribution of charged particles emitted by the carbon nuclei is isotropic for π^{-} absorption but anisotropic for π^{+} absorption; an explanation of this difference is proposed. An energy spectrum of the emitted charged particles in π^{-} absorption is constructed assuming that the particles are protons. The distribution of pion absorption events with respect to the number of star prongs is given. An analysis of these distributions shows that the total $\pi^{\pm}$ energy is in the great majority of cases transferred during the first stage of the absorption process to a pair of internal primary nucleons. This analysis yields 0.65 ± 0.10 for the probability of $\pi^{\pm}$ absorption in carbon nuclei by a neutron-proton pair. The analysis also shows that internal and external (impinging) primary nucleons having equal energies interact differently with nucleons inside carbon nuclei; possible causes of this difference are suggested.

1. INTRODUCTION

AN extensive literature[1-15] now exists regarding $\pi^{\pm}$ meson absorption by different nuclei in a broad energy range. Two stages of the π absorption process can be distinguished. In the first stage the total π energy is transferred to a group of nucleons; the fast nucleons consequently appearing within the nucleus will be called internal primary nucleons. In the second stage the internal primary nucleons interact with other intranuclear nucleons and several particles are emitted.

Most authors agree that in the first stage the total pion energy is transferred within the nucleus mainly to a single pair of nucleons. The probabilities of π^{-} absorption by pairs of either like or unlike nucleons in carbon and aluminum nuclei are determined only in [14]. In [4,7,8,11,13,15] only the probability of absorption by unlike pairs is estimated. Most of the papers contain no information regarding the interaction of internal primary nucleons with other nucleons in the second stage of π absorption. In [15] a Monte Carlo analysis of the experimental results leads to the hypothesis that internal primary nucleons interact with the other nucleons as though the latter were free particles. The Pauli exclusion principle is taken into account and the momentum distribution of intranuclear nucleons is assumed to be that of a nucleon gas.

In the present work we have investigated $\pi^{\pm}$ absorption by carbon at 40—70 MeV. By studying simultaneously the absorption in carbon of pions having opposite charges but identical energies and analyzing the prong distributions we have obtained information regarding the two stages of the absorption process. The prong-number distribution of $\pi^{\pm}$ absorption was based on theoretical distributions depending on four parameters whose values were obtained by least squares using an M-20 electronic computer.

We also obtained the total $\pi^{\pm}$ absorption and charge exchange cross sections for carbon, and have plotted the energy and angle distributions of charged particles emitted during the absorption process. The results are discussed and compared with those of other authors.

2. EXPERIMENTAL PROCEDURE

A rectangular bubble chamber 30 cm long (in the beam direction), 12 cm high, and 10 cm wide was placed behind a 4-meter concrete shield in a $\pi^{\pm}$ beam from the synchrocyclotron of the Joint Institute for Nuclear Research. The $\pi^{\pm}$ mesons were produced in a beryllium target positioned inside the vacuum chamber of the synchrocyclotron in a 670-MeV proton beam. Figure 1 illustrates the ejection of the $\pi^{\pm}$ beams from the synchrocyclotron and the position of the bubble chamber.
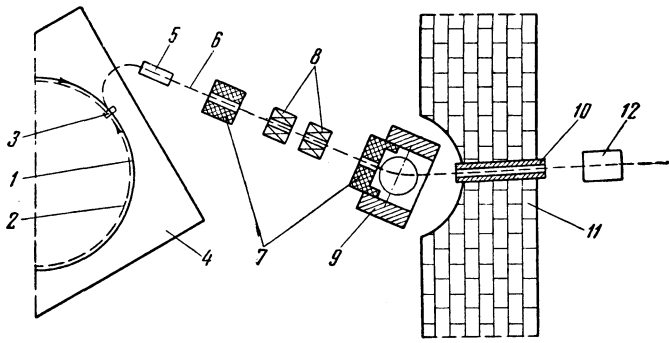
FIG. 1. Experimental arrangement. 1—proton beam for π^+ ejection, 2—proton beam for π^- ejection, 3—beryllium target, 4—synchrocyclotron vacuum chamber, 5—steel fittings connected to yoke of synchrocyclotron electromagnet, 6—$\pi^\pm$ beam, 7—lead shield, 8—quadrupole focusing lenses, 9—deflecting electromagnet, 10—steel collimator, 11—cast iron slabs in window of 4-meter concrete shield, 12—propane bubble chamber.

FIG. 2. Differential distributions of $\pi^\pm$ ranges in propane. $\Delta N^\pm/N^\pm$ is the relative number of $\pi^\pm$ mesons stopping in a 0.8 g/cm² propane range interval. Statistical errors are indicated.

The bubble chamber was placed in a heat bath maintained at 67°C during operation; an initial pressure of 33 atm and 2.6 ± 0.1% expansion were used. The temperature and pressure fluctuations did not exceed ± 0.1°C and ± 0.2 atm, respectively. Charged particle tracks were photographed through the vertical glass of the bubble chamber on film 3.5 cm wide using a stereo camera with two "Yupiter-8" objectives (F = 5.24 cm). The distance from the midplane of the bubble chamber to the film in the camera was 81.2 cm; the separation between the optical axes of the objectives was 12 cm; the photographic base line was vertical. The accelerator was operated continuously; the bubble chamber was operated (under remote control) in a 10-sec cycle. About 2500 stereo photographs each for the π^+ and π^- beams were subjected to stereo scanning.

The $\pi^\pm$ energies in the beam were determined from the differential range curves obtained with the bubble chamber and also independently using a "star detector." [16] Figure 2 shows the differential $\pi^\pm$ range curves in propane (obtained using the bubble chamber). While these curves were being recorded a polyethylene filter 10 cm thick was positioned very close to the bubble chamber in the π beam path. The distributions of π^+ and π^- mesons in propane were practically identical, with a mean energy of 84 MeV and ± 6 MeV spread at half maximum.

Carbon nuclei absorb $\pi^\pm$ mesons in the reaction

$$\pi^\pm + C_6^{12} \rightarrow X, \tag{1}$$

where X is a system containing no particles lighter than a nucleon. The reaction (1) is outwardly mani-
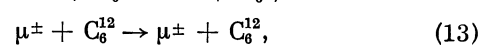
fest by a sharp bend or branching of the particle track, or by the disappearance of the particle when the track terminates in the chamber without exhibiting the bubble density associated with stopping. Many other processes are induced by $\pi^\pm$ mesons or by the admixtures of electrons, positrons, or $\mu^\pm$ mesons in the beam. These processes include

$$\pi^\pm + C_6^{12} \rightarrow \pi^0 + Y, \tag{2}$$

$$\pi^- + p \rightarrow \pi^0 + n, \tag{3}$$

$$\pi^+ \rightarrow \mu^+ + \nu \rightarrow e^+ + \tilde{\nu} + \nu + \nu, \tag{4}$$

$$\mu^\pm \rightarrow e^\pm + \nu + \tilde{\nu}, \tag{5}$$

$$\pi^\pm + e^- \rightarrow \pi^\pm + e^-, \tag{6}$$

$$\mu^\pm + e^- \rightarrow \mu^\pm + e^-, \tag{7}$$

$$e^\pm + e^- \rightarrow e^\pm + e^-, \tag{8}$$

$$\pi^\pm + p \rightarrow \pi^\pm + p, \tag{9}$$

$$\mu^\pm + p \rightarrow \mu^\pm + p, \tag{10}$$

$$e^\pm + p \rightarrow e^\pm + p, \tag{11}$$

$$\pi^\pm + C_6^{12} \rightarrow \pi^\pm + C_6^{12}, \tag{12}$$
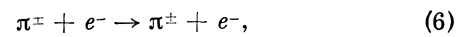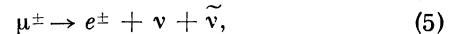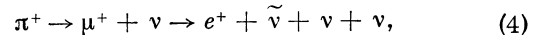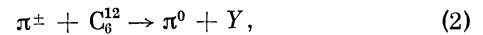
$$\mu^\pm + C_6^{12} \rightarrow \mu^\pm + C_6^{12}, \tag{13}$$

$$e^\pm + C_6^{12} \rightarrow e^\pm + C_6^{12}, \tag{14}$$

$$\pi^\pm + C_6^{12} \rightarrow \pi^\pm + Y. \tag{15}$$
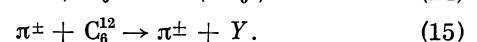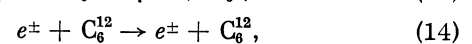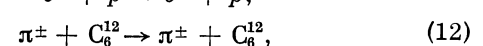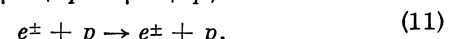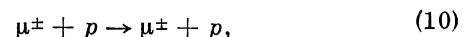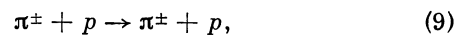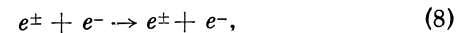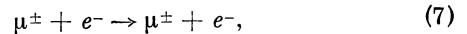
In (2) and (15) Y represents a group of nucleons and heavier particles or an excited C_6^{12} nucleus.

Processes (2)—(15) differ from $\pi^\pm$ absorption by carbon in that they finally yield particles lighter than a nucleon. The definite isolation of type (1) events was based on the detection or nondetection of such particles at the end of a process. Sometimes the tracks of particles lighter than a nucleon at the end of a process are detected in stereo scanning through specific identifying signs. This occurs when electrons or positrons are strongly scattered or when $\mu^\pm$ or $\pi^\pm$ mesons are stopped in the propane bubble chamber. In other cases the events

were further examined using a reprojector and microscope. In reprojection, track lengths and angles were measured in spherical coordinates with the z axis along the beam path through the bubble chamber. Corrections were introduced for track-length and angle distortions resulting from film shrinkage and refraction in propane. The relative densities of bubbles along tracks at the beginning and end of a process were determined microscopically. In each separate case the particle energy at the beginning of a process was calculated assuming the particle to be a pion.

Process (9) was identified using the kinematic relations for all two-prong events. In other events where one or more ionizing particles left the bubble chamber track lengths were used to determine the minimum total kinetic energy of all particles at the end of the process. The energy of separation of the particles from the carbon nucleus was taken into account on the basis of two different hypotheses: (1) that all tracks at the end of a process were formed by protons, and (2) that the track marked by the smallest bubble density of all tracks leaving the chamber belonged to a pion while all other tracks represented protons. It was considered that the interaction was not accompanied by pion absorption if the minimum total energy of all particles at the end of the process on the first hypothesis exceeded the total pion energy at the start of the process. If the minimum total energy of all particles at the termination of the process on the second hypothesis exceeded the pion kinetic energy at the start, the event was assigned to pion absorption by carbon.

In cases where the energy balance did not yield a definite result, the processes that produced ionizing particles leaving the bubble chamber were assigned to a group of unidentified events. The remaining events with tracks ending in the bubble chamber or disappearing can belong only to types (1)−(3). It was impossible to distinguish types (2) and (3) among these because of the low probability that electron-positron pairs are formed in propane by γ quanta from π^0 decay (the radiation length in propane is 104 cm). Therefore the selected events represent the aggregate of processes (1)−(3).

The stereo photographs were subjected to two independent scannings. We examined only events located at least 1 cm from the inside walls of the bubble chamber and not more than 20 cm from the entrance point of the particle into the propane. The $\pi^{\pm}$ energy at the beginning of the working region was 70 MeV; at the end it was 40 MeV. The first scanning for π^+ beams detected 372 events of types (1) and (2); the second scanning added 15

events. For π^- beams 306 events of (1)−(3) were detected at first; 16 were later added. After the two scannings 39 and 27 events remained unidentified in the cases of π^+ and π^- beams, respectively. If it is assumed that the probability of detecting an event is of random character, the efficiency of event registration is 96% for π^+ beams and 95% for π^- beams. Given this efficiency of event detection, two scannings would register 99.8% of all processes (1) and (2) by π^+ beams, and 99.7% of all processes (1)−(3) induced by π^- beams.

3. EXPERIMENTAL RESULTS AND DISCUSSION

A. <u>Total cross section for $\pi^{\pm}$ absorption and charge exchange in carbon at 40−70 MeV.</u> As already stated, the selected events were a combination of processes (1) and (2) for π^+ mesons, and of (1)−(3) for π^- mesons. The number of events representing processes (3) can be determined from the data in the literature regarding the cross sections for this process at 30−65 MeV.[17−19] In the present work the cross section σ_3^- for (3) was taken to be 10 ± 1.5 mb.

The number of events representing process (2) cannot be determined because an accurate experimental cross section has not been obtained. We therefore determined the total cross sections $\sigma_{1,2}^+$ and $\sigma_{1,2}^-$ for (1) and (2) with π^+ and π^- beams, respectively. For this purpose we determined the propane density and the $\mu^{\pm}$, electron, and positron impurities in the beams traversing the bubble chamber. The propane density was found to be $\rho = 0.441 \pm 0.001$ g/cm^3 at 67°C and at the pressure that existed following propane expansion as the beam passed through the bubble chamber. The $\mu^{\pm}$ impurity relative to the number of $\pi^{\pm}$ mesons at the point where the beam leaves the propane is $\gamma_{\mu}^+ = 18 \pm 2\%$ and $\gamma_{\mu}^- = 36 \pm 3\%$ for π^+ and π^-, respectively. The electron and positron impurities relative to the total number of beam particles at the exit from the propane were $\gamma_e^- = 24 \pm 4\%$ and $\gamma_e^+ = 0.5 \pm 0.3\%$.

The foregoing values of $\gamma_e^{\pm}$ and $\gamma_{\mu}^{\pm}$ were used to calculate the total length of $\pi^{\pm}$ tracks in the defined working region of the bubble chamber. For this purpose the track lengths of all particles were measured in each one-tenth part of the stereo photographs. From these data and the numbers $S^{\pm}$ of events (1) and (2) for $\pi^{\pm}$ beams we determined the following cross sections, corrected for detection efficiency:

$$\sigma_{1,2}^+ = 98^{+17}_{-10} \text{ mb}, \qquad \sigma_{1,2}^- = 99^{+24}_{-19} \text{ mb}.$$

In calculating the errors of the cross sections we

took into account the inaccuracies of ρ, $\gamma_\mu^\pm$, $\gamma_e^\pm$, $S^\pm$, and also the errors in determining the number of carbon nuclei per cm^3 of technical propane, the number of particles entering the working volume of the bubble chamber, and track lengths. Unidentified events were included in arriving at the upper error of the cross sections.

For the purpose of testing the correctness of the total $\pi^\pm$ track length obtained in the defined region of the bubble chamber we also obtained the total cross sections $\sigma_{9\,tot}^\pm$ for elastic $\pi^\pm$ scattering in hydrogen [process (9)]. These cross sections for proton track lengths $\geq$ 1 mm were

$$\sigma_{9\,tot}^+ = 12.1\,^{+1.8}_{-1.7}\,mb,\quad \sigma_{9\,tot}^- = 0.6\,^{+0.5}_{-0.3}\,mb\,.$$

The values of $\sigma_{9\,tot}^\pm$ are consistent with the experimental findings in [19-22] for 33—70-MeV $\pi^\pm$ mesons. This indicates that the values of $\sigma_{1,2}^\pm$ do not include any gross errors resulting from inaccurate determination of the total $\pi^\pm$ track length in the chamber. The equality of $\sigma_{1,2}^+$ and $\sigma_{1,2}^-$ obtained for identical $\pi^\pm$ energies is in accord with the charge symmetry hypothesis for nuclear forces.

B. Type (1) events versus number of prongs. Each ionizing-particle track that was at least 2 mm long at the end of the process was counted as a prong. With this definition of prongs, in the experiments with π^+ beams we observed events of types (1) and (2) with from 0 to 4 prongs; in the case of π^+ mesons we observed events of types (1)—(3) with from 0 to 3 prongs. Type (3) can easily be excluded from the experimental prong distribution of events because this process is manifested only by the disappearance of a π^- track and its cross section is sufficiently well known.

Events of types (1) and (2) cannot be separated rigorously because we do not at present have sufficiently complete experimental data regarding type (2). However, a crude error will not be incurred if all events manifested by π^- disappearances are assigned to type (2), which should be observed mainly in this way. This procedure is justified by the fact that our cross section for π^+ disappearance, $\sigma_{dis}^+ = 3.8\,^{+1.3}_{-1.2}\,mb$, is consistent with the cross section for process (2) in [23]. Types (1) and (2) induced by π^- beams were separated assuming that process (2) occurs with zero prongs and that its cross section is the same as with π^+ beams. Figure 3 shows the prong distributions of type (1) events for π^+ and π^- beams. These distributions are characterized by the average prong number $\bar{i}^+ = 2.22\,^{+0.13}_{-0.11}$ for π^+ and $\bar{i}^- = 0.94\,^{+0.14}_{-0.13}$ for π^-.
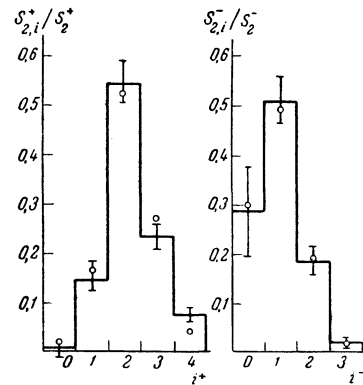

FIG. 3. Distribution of interactions accompanied by $\pi^\pm$ absorption as a function of the number of prongs i having lengths > 2 mm. The indicated errors are based on statistical errors and unidentified events. Calculated values are denoted by circles.

C. Mean proton energy in type (1) events as a function of the number of prongs. It is known from [9] that when stopped π^- mesons are absorbed by nitrogen nuclei the great majority of the produced α particles have energies up to 15 MeV. If it is assumed that in the case of 40—70-MeV $\pi^\pm$ absorption by carbon the majority of α particles have energies in this same range, the α tracks will not be considered prongs because their lengths in propane will not exceed 0.5 mm. Therefore the ionizing-particle tracks registered as prongs belong to lighter singly-charged particles. Since the experimental procedure does not enable us to distinguish these particles, it was therefore assumed that all the prongs were proton tracks. With this hypothesis prong lengths were used to determine the energies of particles stopping in the bubble chamber and the lower energy limit of particles leaving the chamber. The data were then used to calculate the mean minimum proton energy $\bar{T}_{min}$ in type (1) events as a function of the number of prongs. The results are given in Table I, which also includes the mean maximum proton energy $\bar{T}_{max}$, which was determined by taking 90 MeV as the energy of particles leaving the bubble chamber. When the kinetic energy of all particles forming tracks, taking account of their energy of separation from the carbon nucleus, exceeded the total $\pi^\pm$ energy, the total energy of emerging protons was determined from the energy balance.

Using the measurements of particle energies based on prong lengths in the bubble chamber, we plotted the proton energy spectrum in type (1) events for π^- beams (Fig. 4). The distortions of this spectrum resulting from protons leaving the bubble chamber were disregarded, because only

Table I

$\overline{T}$, MeV/prong	π^+-mesons				π^--mesons		
	$i = 1$	2	3	4	$i = 1$	2	3
$\overline{T}_{min}$	46	49	34	26	31	26	20
$\overline{T}_{max}$	57	62	40	28	37	30	20
$\overline{T}_{calc}$	64	53	37	27.5	35	27	23

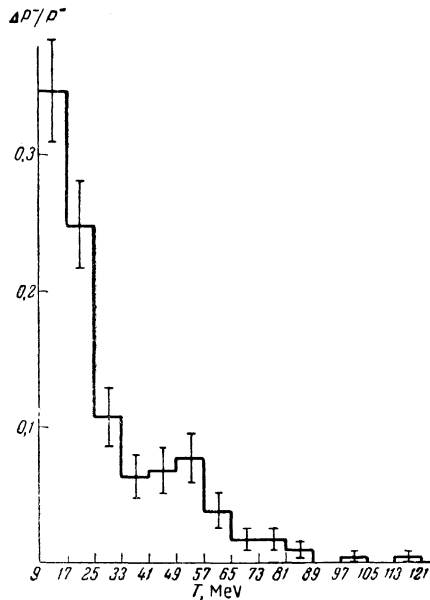FIG. 4. Proton energy spectrum in π^- absorption by carbon. T−proton kinetic energy; $\Delta P/P^-$−relative number of protons in 8-MeV energy interval (with statistical errors).

FIG. 5. Angular distribution of prongs in identified events accompanying $\pi^\pm$ absorption by carbon. $\Delta P^\pm/P^\pm$−relative number of prongs in 30° interval (with statistical errors).

a small number of such protons were included. For π^+ beams these distortions of the proton energy spectrum cannot be neglected because of the large number of particles leaving the chamber. We therefore do not show here the proton energy spectrum obtained with π^+ beams.

D. Angular distributions of prongs in type (1) events. Figure 5 shows the distributions of prongs in identified type (1) events with respect to the angle ϑ, which is the projection of the angle θ between the $\pi^\pm$ tracks and the particle track at the end of the process on a plane parallel to the film plane. The angular distributions of the prongs are seen to differ greatly. This difference is characterized quantitatively by the anisotropy a

$= (P_f - P_b)/(P_f + P_b)$, where P_f and P_b are the total numbers of prongs in the forward and backward hemispheres, respectively, relative to the $\pi^\pm$ direction. The anisotropy for all identified events induced by π^+ beams was $a^+ = 0.164 \pm 0.034$, while for π^- beams it was $a^- = 0.030 \pm 0.065$. In order to obtain the anisotropy as a
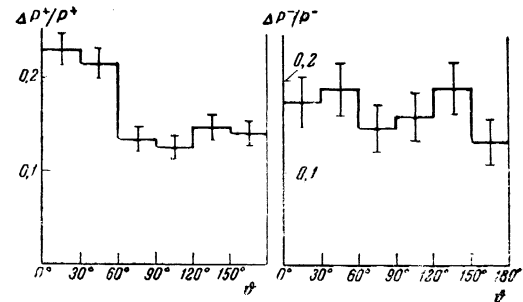
function of the number i of prongs, we calculated $a_i^\pm$ for events with different numbers of prongs. Table II shows the results and the statistical errors as well as values of the anisotropy given in [10,11].

In [10] it was suggested that one of the principal causes of the observed anisotropy is the knocking out of protons from carbon nuclei by the π^+ mesons before the latter are absorbed. To test this hypothesis we determined the cross section σ_{inel} for inelastic π^+ scattering by carbon accompanied by the emission of protons having ranges ≥ 2 mm in propane. The upper limit of σ_{inel} was 6 mb. The number of absorption events accompanied by protons with ranges ≥ 2 mm in propane which were knocked out of carbon nuclei by π^+ mesons before absorption thus does not exceed 1% of all absorption events. This process can therefore not be the main source of the observed anisotropy.

The anisotropy of protons emitted by carbon nuclei in the process of π^+ absorption appears to have two principal causes:

1. In the c.m. system of a π^+ meson and the pair of like nucleons absorbing it, internal primary protons are ejected with higher probability into the forward hemisphere about the π^+ direction. This can be seen by considering the reaction $n + p \rightarrow \pi^+ + n + n$, which is the inverse of π^+ absorption by a pair of like nucleons. In the c.m. system of colliding nucleons in this reaction the π^+ mesons are here emitted with greater proba-

Table II

Source	i				
	1	2	3	4	Mean
π^+- mesons					
Present work	0.113±0.136	0.129±0.050	0.213±0.061	0.204±0.094	0.164±0.034
[10]	1.00—0.56	$0.36^{+0.09}_{-0.10}$	0.36±0.08	0.18±0.09	0.29±0.05
[11]	0.250±0.199	0.130±0.073	0.095±0.077	0.071±0.108	0.110±0.045
π^-- mesons*					
Present work	0.055±0.089	0.011±0.104	—0.067±0.258	—	0.030±0.065

*The corresponding data are lacking in [10,11].

bility in the backward hemisphere about the incident neutron direction.

2. Because of the incident π^+ momentum, protons are ejected from carbon nuclei with higher probability in the forward hemisphere about the π^+ direction.

The foregoing sources of anisotropy should also exist in the case of π^- absorption by carbon. However, the anisotropy of internal primary protons resulting from the first cause should have opposite signs for π^+ and π^- absorption, respectively. This leads to different signs for the anisotropy of charged particles resulting from the first and second causes in the case of π^- absorption. As a result the total anisotropy of charged particles in π^- absorption should be smaller than for π^+ absorption.

Figure 6 shows, for π^+ beams, the distribution of type (1) events with two prongs as a function of the angle β between the prongs. The observed maximum at $\beta \sim 150°$ can be accounted for by as-
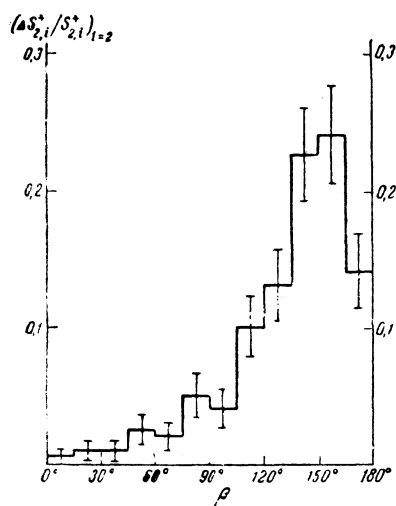

FIG. 6. Two-prong events accompanying π^+ absorption by carbon nuclei vs the angle β between the prongs. $\Delta S_{2,i}^+$, i i = $_2/S_2^+$, i = 2 is the relative number of events in a 15° interval for prong lengths ≥ 2 mm.

suming that pions are absorbed by nucleon pairs in the carbon nucleus.

4. ANALYSIS OF PRONG DISTRIBUTION IN TYPE (1) EVENTS

The number of prongs in type (1) events depends on three factors:

1) The probability of prong formation by charged particles resulting from $\pi^±$ scattering before absorption by carbon nuclei.

2) The qualitative and quantitative compositions of groups of internal primary nucleons receiving the total $\pi^±$ energy in the first stage of the absorption process.

3) The probability of prong formation by charged particles due to a single internal primary nucleon in the second stage of $\pi^±$ absorption by carbon.

In order to simplify the analysis of the type (1) event distribution as a function of the number of prongs, we now make several assumptions regarding the foregoing three factors.

1. We neglect the formation of prongs by charged particles resulting from $\pi^±$ scattering before absorption by carbon. This approximation is based on the fact that the number of these events, as already indicated, does not exceed 1% of all type (1) events.

2. We assume that the total $\pi^±$ energy in the first stage of absorption is transferred only to nucleon pairs. This assumption is based on the results obtained in most investigations of $\pi^±$ absorption by different nuclei.

3) We confine ourselves to processes in which the following particles are emitted from carbon nuclei in the second stage of the $\pi^±$ absorption process:

For each internal primary proton	For each internal primary neutron
a) one proton	a′) one neutron
b) one neutron	b′) one proton
c) a proton and a neutron	c′) a proton and a neutron
d) two protons	d′) two neutrons

Since the experimental technique does not enable us to distinguish between tracks of different singly-charged particles, any other singly-charged particle could take the place of a proton in the foregoing lists. Processes involving particles of greater than unit charge are not considered, because the tracks of such particles in type (1) events are not classified as prongs, as already stated, since their lengths are shorter than 2 mm. Nor do we consider processes in which more than two particles are emitted for each internal primary nucleon; the absence of type (1) events with more than 4 or more than 3 prongs, respectively, for π^+ and π^- beams shows the low probability of these processes. For the same reason we do not consider the process in which a carbon nucleus emits two protons for a single internal primary neutron.

Subject to the indicated assumptions we have the following expressions for the probabilities $W_i^{\pm}$ of type (1) events with i prongs:

$$W_0^+ = 25\eta^+\varkappa^2 (1 - 5\xi - 5\zeta)^2$$
$$+ (1 - \eta^+) [4\varkappa (1 - 6\varkappa) (1 - 6\xi - 4\zeta)$$
$$\times (1 - 4\xi - 6\zeta) + 16\varkappa\zeta (1 - 4\xi - 6\zeta)],$$

$$W_1^+ = \eta^+ [10\varkappa (1 - 5\varkappa) (1 - 5\xi - 5\zeta)^2$$
$$+ 50\varkappa\xi (1 - 5\xi - 5\zeta)]$$
$$+ (1 - \eta^+) [24\varkappa^2 (1 - 6\xi - 4\zeta) (1 - 4\xi - 6\zeta)$$
$$+ (1 - 4\varkappa) (1 - 6\varkappa) (1 - 6\xi - 4\zeta) (1 - 4\xi - 6\zeta)$$
$$+ 24\varkappa\xi (1 - 4\xi - 6\zeta) + 4\zeta (1 - 4\varkappa) (1 - 4\xi - 6\zeta)$$
$$+ 4\xi (1 - 6\varkappa) (1 - 6\xi - 4\zeta) + 16\xi\zeta],$$

$$W_2^+ = \eta^+ [(1 - 5\varkappa)^2 (1 - 5\xi - 5\zeta)^2$$
$$+ 10\xi (1 - 5\varkappa) (1 - 5\xi - 5\zeta)$$
$$+ 50\varkappa\zeta (1 - 5\xi - 5\zeta) + 25\xi^2]$$
$$+ (1 - \eta^+) [6\varkappa (1 - 4\varkappa) (1 - 6\xi - 4\zeta)$$
$$\times (1 - 4\xi - 6\zeta) + 24\varkappa\xi (1 - 6\xi - 4\zeta)$$
$$+ 6\xi (1 - 4\varkappa) (1 - 4\xi - 6\zeta)$$
$$+ 6\zeta (1 - 6\varkappa) (1 - 6\xi - 4\zeta) + 24\zeta^2 + 24\xi^2],$$

$$W_3^+ = \eta^+ [10\zeta (1 - 5\varkappa) (1 - 5\xi - 5\zeta) + 50\xi\zeta]$$
$$+ (1 - \eta^+) [36\varkappa\zeta (1 - 6\xi - 4\zeta) + 36\xi\zeta],$$

$$W_4^+ = 25\eta^+\zeta^2,$$

$$W_0^- = \eta^- [(1 - 5\varkappa)^2 (1 - 5\xi - 5\zeta)^2$$
$$+ 10\zeta (1 - 5\varkappa) (1 - 5\xi - 5\zeta) + 25\zeta^2]$$
$$+ (1 - \eta^-) [6\varkappa (1 - 4\varkappa) (1 - 4\xi - 6\zeta) (1 - 6\xi - 4\zeta)$$
$$+ 36\varkappa\zeta (1 - 6\xi - 4\zeta)],$$

$$W_1^- = \eta^- [10\varkappa (1 - 5\varkappa) (1 - 5\xi - 5\zeta)^2$$
$$+ 50\varkappa\zeta (1 - 5\xi - 5\zeta)$$
$$+ 10\xi (1 - 5\varkappa) (1 - 5\xi - 5\zeta) + 50\xi\zeta]$$
$$+ (1 - \eta^-) [24\varkappa^2 (1 - 4\xi - 6\zeta) (1 - 6\xi - 4\zeta)$$

$$+ (1 - 4\varkappa) (1 - 6\varkappa) (1 - 4\xi - 6\zeta) (1 - 6\xi - 4\zeta)$$
$$+ 6\zeta (1 - 6\varkappa) (1 - 6\xi - 4\zeta)$$
$$+ 6\xi (1 - 4\varkappa) (1 - 4\xi - 6\zeta)$$
$$+ 24\varkappa\xi (1 - 6\xi - 4\zeta) + 36\xi\zeta],$$

$$W_2^- = \eta^- [25\varkappa^2 (1 - 5\xi - 5\zeta)^2$$
$$+ 50\varkappa\xi (1 - 5\xi - 5\zeta) + 25\xi^2]$$
$$+ (1 - \eta^-) [4\varkappa (1 - 6\varkappa) (1 - 4\xi - 6\zeta) (1 - 6\xi - 4\zeta)$$
$$+ 24\varkappa\xi (1 - 4\xi - 6\zeta) + 4\xi (1 - 6\varkappa) (1 - 6\xi - 4\zeta)$$
$$+ 4\zeta (1 - 4\varkappa) (1 - 4\xi - 6\zeta) + 24\xi^2 + 24\zeta^2],$$

$$W_3^- = (1 - \eta^-) [16\xi\zeta + 16\varkappa\zeta (1 - 4\xi - 6\zeta)].$$

The parameters $\eta^{\pm}$, ξ, ζ, and κ have the following meanings: $\eta^{\pm}$ is the probability that the total $\pi^{\pm}$ energy is transferred in the first stage of the absorption to a pair of unlike nucleons; according to hypothesis (2), the quantity $1 - \eta^{\pm}$ is the probability that the total $\pi^{\pm}$ energy is transferred to a pair of like nucleons in the first stage. ξ is the ratio of the probability of process c (c') to the number of neutrons (protons) in the core of the nucleus. ζ is the ratio of the probability of process d (d') to the number of protons (neutrons) in the core. κ is the ratio of the probability of process b (b') to the product of the sum of the probabilities of processes a and b (a' and b') by the number of neutrons (protons) in the core.

The expressions for $W_i^{\pm}$ will now be explained by comparison with W_0^+. The total π^+ energy is transferred in the first stage of absorption to a pair of unlike nucleons with probability η^+. The carbon nucleus then contains two fast internal primary protons and a core consisting of five protons and five neutrons. Type (1) events with zero prongs will be observed only if a neutron is emitted for each internal primary proton. The probability of this event will be $\eta^+ [5\kappa(1 - 5\xi - 5\zeta)]^2$. The total π^+ energy is transferred in the first stage of absorption to a pair of like nucleons with probability $1 - \eta^+$. In this case the carbon nucleus contains a fast internal primary proton and a fast internal primary neutron plus a core consisting of six protons and four neutrons. Type (1) events with zero prongs will be observed only if a neutron is emitted for each internal primary proton, and either one or two neutrons are emitted for each internal primary neutron. In the first case the probability of this event will be $(1 - \eta^+) \times 4\kappa(1 - 4\xi - 6\zeta)(1 - 6\kappa) \times (1 - 6\xi - 4\zeta)$, and in the second case it will be $(1 - \eta^+) \times 4\kappa(1 - 4\xi - 6\zeta) \times 4\zeta$. The probability W_0^+ will obviously equal the sum of all three probabilities.

We can write $\eta^+ = \eta^- = \eta$ in the given expres-

sions for $W_i^{\pm}$ because the proton and neutron distributions in the carbon nucleus evidently having the same dependence on distance from the nuclear center. In order to obtain more complete information regarding the first and second stages of $\pi^{\pm}$ absorption by carbon nuclei it is of interest to determine the parameters η, ξ, ζ, and κ as functions of the minimum prong length. For this purpose we plotted the distributions of type (1) events with regard to the numbers of prongs having minimum lengths of 4, 5, 6, 7, and 11 mm. The stated parameters were then determined by least squares for each distribution. Figure 7 shows the dependences of these parameters on the kinetic energy T_{min} of protons whose ranges in propane equalled the minimum prong lengths 2, 4, 5, 6, 7, and 11 mm. For these minimum prong lengths the weighted sums of the square deviations χ^2 of experimental from theoretical values of $W_i^{\pm}$ are 9.7, 1.6, 0.8, 3.2, 4.3, and 5.2, respectively. A comparison with the mean $\chi^2 = 5$ of the χ^2 distribution indicates that the foregoing hypotheses regarding the influence of the different factors on the number of prongs in type (1) events do not disagree with experiment.
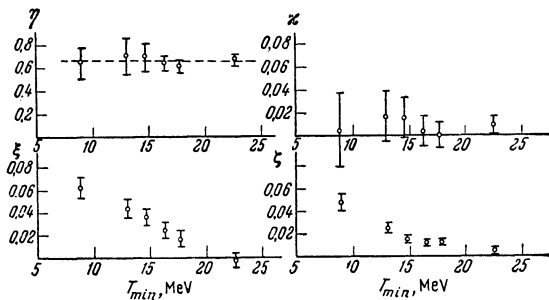

FIG. 7. The parameters η, ξ, ζ, and κ vs. the kinetic energy T_{min} of a proton having a range in propane that is equal to the minimum prong length.

5. ANALYSIS OF DEPENDENCES OF MEAN PROTON ENERGY IN TYPE (1) EVENTS ON NUMBER OF PRONGS

Keeping in mind the hypotheses regarding the influences of different factors on the number of prongs i in type (1) events, we can write expressions for the mean proton energy $T_i^{\pm}$ in these events using the additional notation:

1) U_1 for the effective proton energy in processes a and b';

2) U_2 for the effective proton energy in process c;

3) U_3 for the effective proton energy in process c'.

Since the protons in process d cannot be dis-

tinguished we can speak only of the combined energy of both protons, which approximately equals the sum of the effective energies U_2 and U_3.

It is easily seen that the expressions for $T_i^{\pm}$ are functions of seven parameters: $T_i^{\pm} = F_i (\eta, \xi, \zeta, \kappa, U_1, U_2, U_3)$; of these U_1, U_2, and U_3 are unknown. In the present work values of these three unknown parameters were obtained from three equations for $\overline{T_3^+}$, $\overline{T_1^-}$, and $\overline{T_2^-}$. We assumed $\xi = \zeta = 0.055$ and $\kappa = 0$ in order to simplify the calculations. Several groups of values of U_1, U_2, and U_3 were obtained within the limits for $\overline{T_3^+}$, $\overline{T_1^-}$, and $\overline{T_2^-}$. For each set of values of U_1, U_2, and U_3 the mean proton energies $\overline{T_1^+}$, $\overline{T_2^+}$, $\overline{T_4^+}$, and $\overline{T_3^-}$ were calculated. The best agreement with experiment was obtained using effective proton energies within the following limits: $U_1 = 65-75$ MeV, $U_2 = 39-46$ MeV, and $U_3 = 14-16$ MeV. Table I gives the calculated mean proton energies in type (1) events for the parameters $U_1 = 75$ MeV, $U_2 = 41$ MeV, and $U_3 = 14$ MeV.

6. DISCUSSION OF RESULTS

In Fig. 7 the values of η lie, within experimental error limits, on a straight line at the weighted mean level $\eta = 0.65$. However, a comparison of the distributions of type (1) events with respect to the numbers of prongs having minimum ranges 2 and 11 mm (shown in Figs. 3 and 8, respectively) indicates that these distributions are highly deformed as T_{min} is changed. Therefore the observed mutual independence of η and T_{min} denotes that the foregoing hypotheses regarding the influences of the different factors on the number of prongs in type (1) events reflect mainly correctly the physics of $\pi^{\pm}$ absorption by carbon nuclei. Ac-
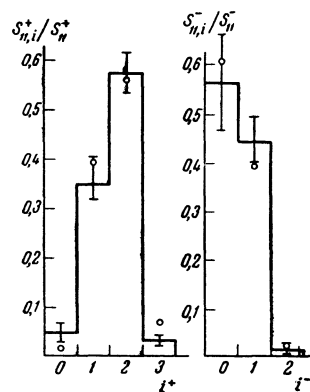

FIG. 8. Events accompanied by $\pi^{\pm}$ absorption vs. the number of prongs having minimum lengths ≥ 11 mm. The indicated errors are due to statistical errors and unidentified events. Circles denote calculated values.

cordingly, all distributions of type (1) events versus the number of prongs may be characterized, independently of T_{min}, by a single weighted mean η = 0.65 ± 0.10. The error $\Delta\eta$ was not calculated as the error $\Delta\eta_1$ of the weighted mean, but from the formula $\Delta\eta = \sqrt{(\Delta\eta_1)^2 + (\Delta\eta_2)^2}$, where $\Delta\eta_2$ is the mean error of η for different values of T_{min}. The value obtained for η agrees with [5] but disagrees somewhat with [14]; the discrepancy could result from different pion energies in the different investigations.

Figure 7 shows that ξ and ζ vanish at T_{min} ~ 25 MeV. This indicates that one of the two nucleons emitted in processes c, c', d or d' has energy not exceeding 25 MeV. The energy of the other particle should generally exceed 25 MeV; otherwise χ^2 would be observed to increase with increasing minimum prong length. The values of U_2 and U_3 are consistent with these results.

Linear extrapolations show that, for T_{min} = 0, ξ and ζ each reach a value of the order 0.1. This gives some indication that for T_{min} = 0 either the probabilities of processes a and a', or b and b' are close to zero, or that in these processes the residual nucleus is excited in most instances. This conclusion is consistent with the value of U_1. A similar conclusion is derived from the fact that the sum of the average numbers of prongs $\overline{i^+}$ and $\overline{i^-}$ in type (1) events has a value of about 4 for T_{min} = 0, as is shown by the linear extrapolation in Fig. 9. This result is found because the sum is the average number of all particles having energy exceeding T_{min} in type (1) events if the charged particles in these events are assumed to be protons. This result is easily obtained if we retain the foregoing hypotheses regarding the influences of different factors on the numbers of prongs in type (1) events.

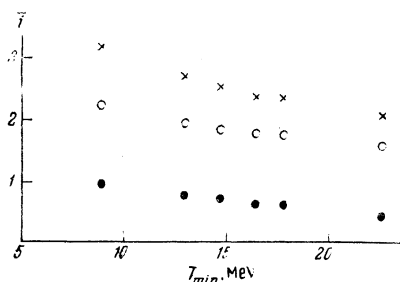In Fig. 7, for all values of T_{min}, κ is zero within the experimental error limits. This indi-

FIG. 9. Average number of prongs vs. kinetic energy T_{min} of a proton having a range in propane equal to the minimum prong length. ●—for interactions accompanying π^- absorption by carbon nuclei; O—the same for π^+ mesons; ×—average number of charged and neutral particles in interactions accompanying $\pi^{\pm}$ absorption by carbon.

cates that of the two unlike nucleons in processes c and c' the larger energy in most cases is possessed by the nucleon that is like the internal primary nucleon. The value of U_2 is consistent with this conclusion. A similar conclusion is reached from a comparison of the experimental and calculated numbers of protons $P^{\pm}$ in the range 9−25 MeV in Table III. The values of $P^{\pm}$ were calculated for three different sets of values of $K^{\pm}(c)$, $K^{\pm}(c')$, and $K^{\pm}(d)$, representing the respective fractions of protons having energies 9−25 MeV in processes c, c', and d:

I. $K^{\pm}(c')) = 1$, $K^{\pm}(c)) = 0$, $K^{\pm}(d)) = 0.5$;

II. $K^{\pm}(c')) = 0.5$, $\quad K^{\pm}(c)) = 0.5$, $\quad K^{\pm}(d)) = 0.5$;

III. $K^{\pm}(c')) = 0$, $\quad\quad K^{\pm}(c)) = 1$, $\quad K^{\pm}(d)) = 0.5$.

Table III

Experiment	Calculation		
	Variant I	Variant II	Variant III
P^+ 199	201	266	332
P^- 138	139	94	50

This table shows that the first variant agrees best with experiment. This result confirms the conclusion derived from the discussion of the dependence of κ on T_{min}.

In the light of the foregoing we can easily account for the energy spectrum of protons emitted by carbon nuclei as a result of π^- absorption (Fig. 4). The observed steep falling-off at 25 MeV is associated with the fact that the great majority of protons have energies under 25 MeV in process c', which is the dominating source of charged particles in π^- absorption.

It is of interest to compare the interaction between nucleons of the carbon nucleus and primary nucleons, both internal and external (impinging), having identical energies. In the present work we can take 97 MeV as the mean energy of internal primary nucleons. The interactions of external primary protons and neutrons with nucleons in carbon nuclei were investigated in [24,25] at about 97 MeV. The resulting energy and angle distributions of the nucleons indicate that external primary neutrons (protons) interact with protons (neutrons) inside carbon nuclei as though the latter were free particles (taking into account the Pauli exclusion principle, the momentum distribution of intranuclear nucleons, and the collisions of secondary nucleons with intranuclear nucleons). If the interactions of internal and external primary nucleons

were identical, we would have obtained in the present work: $\kappa = 0.07$, $U_2 = U_3$, $K^{\pm}(c') = K^{\pm}(c)$ $= K^{\pm}(d) = 0.5$. The fact that our results were different from these shows that external and internal primary nucleons interact differently with nucleons inside carbon nuclei. The difference may result from the structure of the carbon nucleus. Indeed, when 55-MeV $\pi^{\pm}$ mesons are absorbed by carbon, the angular distribution of internal primary nucleons about a straight line connecting their centers should be anisotropic. If the carbon nucleus has a structure, this anisotropy should lead to a difference in the angle and energy distributions of nucleons emitted by the carbon nuclei as a result of interactions with external and internal primary nucleons.

The foregoing analysis of the experimental findings differs from the Monte Carlo method, whereby a nuclear model is assumed and the internal primary nucleons are considered as interacting with the remaining nucleons considered as free particles, while taking into account the exclusion principle and the momentum distribution of intranuclear nucleons.

In conclusion the authors wish to express their deep gratitude to B. M. Pontecorvo for his constant interest and valuable suggestions; to M. G. Meshcheryakov, S. S. Gershteĭn, and V. G. Solov'ev for discussions of the results; to Yu. D. Prokoshkin for the extraction of the $\pi^{\pm}$ beams; and to E. P. Zhidkov and A. F. Luk'yantsev for assistance in processing the experimental data on an electronic computer. We also wish to thank V. L. Trifonov and A. I. Sharov for experimental assistance, and E. A. Burov for processing the stereo photographs, as well as the group directed by I. A. Pankov and K. A. Baĭcher for preparing the bubble chamber.

[1] G. Bernardini and F. Levy, Phys. Rev. 84, 610 (1951).

[2] B. Rankin and H. Bradner, Phys. Rev. 87, 553 (1952).

[3] A. Minguzzi and A. Minguzzi-Ranzi, Nuovo cimento 10, 1100 (1958).

[4] A. M. Shapiro, Phys. Rev. 84, 1063 (1951).

[5] Byfield, Kessler, and Lederman, Phys. Rev. 86, 17 (1952).

[6] J. F. Tracy, Phys. Rev. 91, 960 (1953).

[7] Petrov, Ivanov, and Rusakov, JETP 37, 957 (1959), Soviet Phys. JETP 10, 682 (1960).

[8] F. H. Tenney and J. Tinlot, Phys. Rev. 92, 974 (1953).

[9] P. Ammiraju and L. M. Lederman, Nuovo cimento 4, 283 (1956).

[10] Laberrigue-Frolova, Balandin, and Otvinovskiĭ, JETP 37, 634 (1959), Soviet Phys. JETP 10, 452 (1960).

[11] R. G. Salukvadze and D. Neagu, JETP 41, 78 (1961), Soviet Phys. JETP 14, 59 (1962).

[12] Wang, Wang, Ting, Dubrovskiĭ, Kladnitskaya, and Solov'ev, JETP 35, 899 (1958), Soviet Phys. JETP 8, 625 (1959).

[13] Blinov, Lomanov, Shalamov, Shebanov, and Shchegolev, JETP 35, 880 (1958), Soviet Phys. JETP 8, 609 (1959).

[14] Ozaki, Weinstein, Glass, Loh, Neimala, and Wattenberg, Phys. Rev. Letters 4, 533 (1960).

[15] De Sabbata, Manaresi, and Puppi, Nuovo cimento 10, 1704 (1953).

[16] Dunaitzev, Prokoshkin, and Tang, Nuclear Instr. and Meth. 8, 11 (1960).

[17] W. J. Spry, Phys. Rev. 95, 1295 (1954).

[18] J. Tinlot and A. Roberts, Phys. Rev. 95, 137 (1954).

[19] Bodansky, Sachs, and Steinberger, Phys. Rev. 93, 1367 (1954).

[20] S. L. Leonard and D. H. Stork, Phys. Rev. 93, 568 (1954).

[21] C. E. Angell and J. P. Perry, Phys. Rev. 92, 835L (1953).

[22] Orear, Lord, and Weaver, Phys. Rev. 93, 575 (1954).

[23] A. Roberts and J. Tinlot, Phys. Rev. 90, 951 (1953).

[24] J. A. Hofmann and K. Strauch, Phys. Rev. 90, 449 (1953).

[25] J. Hadley and H. York, Phys. Rev. 80, 345 (1950).

Translated by I. Emin
61